Discrete and Continuous Dynamical Systems - Series S
Vol. 17, No. 7, July 2024, pp. 2298-2322
doi:10.3934/dcdss.2024032

OPTIMAL CONTROL OF THERAPIES ON A TUMOR GROWTH MODEL WITH BRAIN LACTATE KINETICS

Laurence Cherfils[*1], Stefania Gatti[2], Alain Miranville[3], Hussein Raad[1] and Rémy Guillevin[3,4]

[1]La Rochelle Université, Laboratoire des Sciences de l'Ingénieur pour l'Environnement UMR CNRS 7356, Avenue Michel Crépeau, F-17042 La Rochelle Cedex 1, France

[2]Università di Modena e Reggio Emilia, Dipartemento di Scienze Fisiche Informatiche e Matematiche, Via Campi 213/B, I-41125 Modena, Italy

[3]Laboratoire I3M et Laboratoire de Mathématiques et Applications, Université de Poitiers Equipe DACTIM-MIS, Site du Futuroscope - Téléport 2, 11 Boulevard Marie et Pierre Curie 86073 Poitiers Cedex 9, France

[4]CHU de Poitiers, 2 rue de la Milétrie, 86000 Poitiers, France

Abstract. We prove the existence of an optimal treatment combining chemotherapy and a lactate targeting drug for a mathematical model for high grade gliomas and lactate kinetics. A necessary condition for a treatment to be optimal is also devised, allowing to design numerically the proper therapy. The analytical results are validated by the numerical simulations; as clinical experience proves, the simulations show that the effect of chemotherapy is enhanced by the other drug whose sole administration is, in turn, almost irrelevant.

1. **Introduction.** Glioblastoma (high grade glioma) is the most common and malignant primary brain tumor in adults, recognized by angiogenesis, invasive growth and necrosis. The current treatment for such tumors consists in surgical resection, followed by concomitant radio-chemotherapy (see [21]). Nevertheless, tumor relapses since invasive cells can not be fully eradicated. Therefore, alternative therapeutic strategies and targets are highly needed.

In this respect, it has been observed that, like other cancers, glioblastoma modifies cell's energy management, a relevant issue for an organ with high energy needs like the brain. In particular, the persistence of aerobic glycosis (the Warburg effect) is a characteristic of cancer cells and the lactate, the end-product of glycolysis, is a hallmark of advanced cancers. Besides, lactate creation, consumption, import and export in glioma cells play a central role in the cancer development (see e.g. [14] and the references therein) and may therefore be considered as a key point for the trail of new therapeutic strategies (see e.g., [6, 24]).

In this paper, we propose a mathematical model coupling the evolution of a high grade glioma cell density with those of the intracellular and capillary lactate

2020 *Mathematics Subject Classification.* 35Q92, 35Q93, 92C50, 65M60, 35K51, 35K58, 49J20, 49K20.

Key words and phrases. Reaction-diffusion equations, lactate kinetics, tumor growth, chemotherapy, well-posedness, optimal control, adjoint equation, numerical simulations.

*Corresponding author: Laurence Cherfils.

concentrations in the brain, when two different therapies are administered: on the one hand, a cytotoxic drug to kill cancer cells; on the other hand, a drug targeting lactate. In this sense, several choices are reported in the clinical literature, each addressed to different aspects of lactate interactions with cancer (see the review paper [6]).

For instance, in [20], the authors emphasize that, disrupting the lactate production and the exchanges by monocarboxylate transporters (MCT1) could become an efficient anticancer treatment in the future. Another strategy for a drastic decrease in tumor development and invasion, devised in [15], consists in the total disruption of lactate dehydrogenase (LDH A and B), achieved by administering an antiepileptic drug (stiripentol); this targets LDH activities (so inhibiting lactate generation) and increases survival in intracranially implanted mice.

Besides, lactate induces angiogenesis therefore its decrease has itself an antiangiogenic effect as it also starves the tumor; on the other hand, an antiangiogenic treatment affects lactate production since it reduces the vascularization that brings nutrients to the tumor. Indeed, recently, anti-angiogenic drugs have been administered together with lactate modulating therapies [24].

We think that our model may account for many of these therapeutic strategies targeting lactates; therefore, in what follows we refer generically to a drug targeting lactate meaning that it can be an antiangiogenic, antiepileptic or other therapy.

Assuming fixed chemotherapy and lactate targeting therapies, the mathematical analysis of this system has already been done in [8]. Still due to the high and dangerous side-effects of these drugs on patients, the minimal quantities to achieve the desired reduction of the tumor should be devised by oncologists. Therefore, in this paper, the therapies are no longer fixed but are viewed as control functions, and the aim is to minimize the cost functional measuring the distance from the desired tumor and lactates concentrations as well as the drugs toxicity, under the constraint of the state evolutionary problem (see the subsequent system (1)). In particular, we analytically prove that an optimal therapeutic strategy exists and we devise a necessary condition for an admissible control to be optimal; this allows to numerically determine an optimal therapy. Then we propose simulations corresponding to different therapeutic schedules for virtual patients. These simulations should further integrate clinical data from MR acquisition on 7Tesla platform (CHU de Poitiers), including lactate quantifications and perfusion values. We expect this approach to be useful for individual patient monitoring, thus allowing anticipation of treatment efficiency and adaptation.

The relation between glioma and lactate has been described by different mathematical models: in particular, we recall [14, 17] for lactate kinetics in a glioma environment and [8] accounting the evolution of both lactate and tumor. Brain tumor therapies were included , e.g., in [4, 11, 22, 23] and the references therein (see also [9, 10, 12] for other cancer therapies). Finally, optimal treatments targeting lactate were studied in [2, 19].

2. **The model.**

The mathematical model analyzed in this paper is given by three parabolic equations for the tumor cell density u, the intracellular lactate concentration φ and the capillary lactate concentration ψ. This system was firstly analysed in [7] for modeling high grade glioma growth submitted to fixed treatments. More precisely, the equations modeling lactate kinetics are based on [3], including the effects of the tumor on lactates as well as a therapy targeting lactate

(antiangiogenic or antiepileptic drug for instance) represented by the function s. In turn, the evolution of the tumor cell density takes into account diffusion through the matrix D and logistic proliferation together with the combined effects of a cytotoxic drug v (Temozolomide) and of the lactate targeting therapy as well as apoptosis and necrosis (see e.g. [1]). The resulting system reads

$$\begin{cases} \partial_t u - \operatorname{div}(D\nabla u) = [a(\varphi+\psi) - p(\mathsf{s})\mathsf{v}]\, u\,(1-u) - ug(\varphi+\psi), & \text{in } \Omega_T, \\ \partial_t \varphi - \alpha\Delta\varphi + k(u,\mathsf{s})\left(\dfrac{\varphi}{K+\varphi} - \dfrac{\psi}{K'+\psi}\right) = \beta(u,\mathsf{s})J, & \text{in } \Omega_T, \\ \epsilon\partial_t \psi - \varrho\Delta\psi + k(u,\mathsf{s})\left(\dfrac{\psi}{K'+\psi} - \dfrac{\varphi}{K+\varphi}\right) = F(u,\mathsf{s})\,[L(u)-\psi]\,, & \text{in } \Omega_T, \\ D\nabla u\cdot\mathbf{n} = \partial_{\mathbf{n}}\varphi = \partial_{\mathbf{n}}\psi = 0, & \text{on } \Sigma_T, \\ u(0) = u_0, \quad \varphi(0) = \varphi_0, \quad \psi(0) = \psi_0, & \text{in } \Omega, \end{cases} \tag{1}$$

where $\Omega_T = \Omega \times (0,T)$ and $\Sigma_T = \partial\Omega \times (0,T)$, Ω being a bounded and regular domain of $\mathbb{R}^N$ with $N = 1, 2, 3$; the vector $\mathbf{n}$ is the unit outward normal to the boundary $\partial\Omega$.

In the tumor equation, the rate a represents the balance between the rates of proliferation and apoptosis whereas necrosis occurs at rate g. Both a and g depend on the sum of the lactate concentrations. Moreover, the tumor net proliferation rate is opposed by the action of the chemotherapy function v, enhanced by the antiangiogenic/antipilectic therapy via the term $p(\mathsf{s})$.

Then, α and ϱ are the positive constant diffusion coefficients of intracellular and capillary lactates, respectively. The positive constant K, K' stand for modified Michaelis-Menten constants (see [3]). Besides, the maximum transport rate of lactate through monocarboxylate transporters $k(u,\mathsf{s})$ increases with the tumor concentration and is decreased by the antiangiogenic/antiepileptic drug in tumor tissue.

The positive constant J collects the cell lactate production by glycolysis, the lactate consumption by metabolism and the lactate diffusion towards the neighbouring regions. The term $\beta(u,\mathsf{s})$ in front of J expresses the fact that the lactate production/diffusion/consumption is enhanced by the tumor, but is also subject to the antiangiogenic/antiepileptic treatment.

The rate of change of capillary lactate ψ is influenced by the small positive constant ϵ corresponding to the ratio of the volume fraction of capillary compartment over that of intracellular space. On the right-hand side of the balance equation for ψ, we have the difference of lactate input to capillaries and output from capillaries: in particular, the cerebral blood flow $F(u,\mathsf{s})$, accessible by perfusion MRI, is influenced by the tumor and is opposed by the antiangiogenic/antiepileptic drug s. The resulting flux takes into account the arterial lactate concentration $L(u)$.

Our aim in this paper is to control the treatments v and s in order to reduce the tumor and lactate concentrations, up to desired targets. Hence we intend to minimize the following functional:

$$\begin{aligned} &\mathcal{J}(u,\varphi,\psi,\mathsf{v},\mathsf{s}) \\ &= \frac{k_1}{2}\int_{\Omega_T} [u(x,t) - u_Q(x,t)]^2\,dxdt + \frac{k_2}{2}\int_{\Omega} [u(x,T) - u_\Omega(x)]^2\,dx + k_3\int_{\Omega} u(x,T)\,dx \end{aligned}$$

$$+\frac{k_4}{2}\int_{\Omega_T}[\varphi(x,t)+\psi(x,t)-\ell_Q(x,t)]^2\,dxdt$$
$$+\frac{k_5}{2}\int_{\Omega}[\varphi(x,T)+\psi(x,T)-\ell_\Omega(x)]^2\,dx$$
$$+\frac{k_6}{2}\int_{\Omega_T}\mathsf{v}^2(x,t)\,dxdt+\frac{k_7}{2}\int_{\Omega_T}\mathsf{s}^2(x,t)\,dxdt.$$

Here the constant k_1, k_2, ... k_7 are nonnegative, while the functions u_Ω and u_Q refer to prescribed targets for tumor densities in Ω and Ω_T respectively. In the same way, ℓ_Ω et ℓ_Q stand for prescribed targets of the sum of lactate concentrations in Ω and Ω_T. We emphasize that today, neuroimaging techniques allow an indirect and noninvasive measure of lactate concentrations in healthy and cell tumors, but only the total lactate concentrations can be measured, corresponding to $\varphi+\psi$. The last two terms of $\mathcal{J}$ penalize large quantities of drugs so rendering their toxicity.

2.1. **Assumptions and functional setting.** Complying with the biological meaning of the aforementioned functions, we assume that

(H1) the proliferation rate $a\in C^1(\mathbb{R})$ is such that $0<\mathsf{a}_1\le a(\phi)\le\mathsf{a}_2$ for any $\phi\in\mathbb{R}$. Moreover, a and a' are Lipschitz continuous in $\mathbb{R}$ with $a'\in L^\infty(\mathbb{R})$.

(H2) the necrosis rate $g\in C^1(\mathbb{R})$ is such that $0\le g\le\mathsf{G}$. Moreover, g and g' are Lipschitz continuous in $\mathbb{R}$ with $g'\in L^\infty(\mathbb{R})$.

(H3) the function L, representing the arterial lactate concentration, is $L\in C^1(\mathbb{R})$ monotone increasing with $L(0)\ge 0$. Moreover L and L' are Lipschitz continuous.

(H4) the matrix D is symmetric and there exists $d>0$ such that $(D\xi,\xi)\ge d|\xi|^2$, $\forall\xi\in\mathbb{R}^3,\quad \xi\neq 0$.

(H5) the cytotoxic and antiangiogenic/antiepileptic drugs are described by $\mathsf{v},\mathsf{s}\in L^\infty(\Omega_T)$.

(H6) the function β is defined by $\beta(u,\mathsf{s})=\beta_0+\mathrm{b}(\mathsf{s})u$, where $\beta_0\ge 0$ is constant and $\mathrm{b}\in C^1(\mathbb{R})$ is nonnegative. Moreover, b and b$'$ are Lipschitz continuous in $\mathbb{R}$.

(H7) the function F representing the cerebral blood flux is defined by $F(u,\mathsf{s})=F_0+\mathrm{F}(\mathsf{s})u$, where $F_0>0$ is constant while $\mathrm{F}\in C^1(\mathbb{R})$ is nonnegative and Lipschitz continuous in $\mathbb{R}$ together with F$'$.

(H8) the maximal transport rate of the monocarboxylate transporters k is defined by $k(u,\mathsf{s})=\kappa_0+\mathrm{k}(\mathsf{s})u$, where $\kappa_0\ge 0$ is constant and $\mathrm{k}\in C^1(\mathbb{R})$ is nonnegative. Moreover, k and k$'$ are Lipschitz continuous in $\mathbb{R}$.

(H9) the function p, accounting for the action of the antiangiogenic/antiepilectic therapy on the tumor, belongs to $C^1(\mathbb{R})$ and is Lipschitz continuous with p'.

We set $H=L^2(\Omega)$ with inner product denoted by $(\cdot,\cdot)$ and corresponding norm $\|\cdot\|$. This space will give a Hilbert triplet together with $V=H^1(\Omega)$ equipped with the norm $\|u\|_V^2=\|u\|^2+\|\nabla u\|^2$ and its dual space V', the symbol $\langle\cdot,\cdot\rangle$ standing for the corresponding duality pairing. Notice that we do not make any difference between scalar products and norms in H and H^3. Also, given a matrix $\mathbb{M}=(m^i_j)\in\mathcal{M}_3(\mathbb{R})$ and a vector $U=(U_1,U_2,U_3)\in\mathbb{R}^3$, leaving the transpose unexpressed, we just write

$$\mathbb{M}U=\left(\sum_{j=1}^3 m^i_jU_j\right)\qquad\text{and}\qquad \mathbb{M}UV=\sum_{i,j=1}^3 m^i_jU_jV_i,\quad\forall V=(V_1,V_2,V_3)\in\mathbb{R}^3.$$

Considering triplets accounting for the tumor cell density and the two lactate concentrations, we then introduce

$$\mathcal{H} = H^3 \qquad \text{and} \qquad \mathcal{V} = V^3, \quad \text{with dual space} \quad \mathcal{V}'.$$

Actually, the proper phase space for biologically meaningful solutions is a subset of $\mathcal{H}$, that is,

$$\mathcal{H}^+ = H^{++} \times H^+ \times H^+,$$

where

$$H^+ = \{v \in H : \ v \geq 0 \text{ a.e. in } \Omega\} \quad \text{and} \quad H^{++} = \{v \in H : \ 0 \leq v \leq 1 \text{ a.e. in } \Omega\}.$$

2.2. **Known results at fixed therapies.** We now assume that the functions v and s, representing the cytotoxic and antiangiogenic/antiepileptic drugs respectively, meeting (H5) are fixed.

Besides, for the sake of simplicity, we set $\epsilon = \alpha = \varrho = 1$. Under assumptions weaker than (H1)–(H9), we showed in [7]

Theorem 2.1. *For given $T > 0$, assume that (v, s) satisfying (H5) are fixed. Then for any fixed $z_0 = (u_0, \varphi_0, \psi_0) \in \mathcal{H}^+$ there exists a weak solution $z = (u, \varphi, \psi)$ to (1) on $(0, T)$. In particular, $z(t) \in \mathcal{H}^+$ for almost any $t \in (0, T)$ and satisfies*

$$\|z\|^2_{L^2(0,T;\mathcal{V})\cap C([0,T];\mathcal{H})\cap H^1(0,T;\mathcal{V}')} \leq c(\|z_0\|^2_{\mathcal{H}} + \|\mathsf{v}\|^2_{L^2(0,T;H)} + \|\mathsf{s}\|^2_{L^2(0,T;H)} + 1), \quad (2)$$

for some positive constant c depending on T and on the problem parameters.

Moreover, given $(\mathsf{v}_i, \mathsf{s}_i)$ satisfying (H5) and $z_{0i} \in \mathcal{H}^+$ $(i = 1, 2)$, if z_i is a weak solution to (1) corresponding to $(\mathsf{v}_i, \mathsf{s}_i)$ with initial data z_{0i}, then there exists $c > 0$, depending on T and on the problem structural data, such that

$$\begin{aligned} &\|z_1(t) - z_2(t)\|^2_{\mathcal{H}} + \|z_1 - z_2\|^2_{L^2(0,T;\mathcal{V})} \qquad (3)\\ &\leq c(\|z_{01} - z_{02}\|^2_{\mathcal{H}} + \|\mathsf{v}_1 - \mathsf{v}_2\|^2_{L^2(0,T;H)} + \|\mathsf{s}_1 - \mathsf{s}_2\|^2_{L^2(0,T;H)}), \end{aligned}$$

for any $t \in [0, T]$. As a consequence, the solution to (1) with fixed initial datum and therapies is unique.

If we further assume $\varphi_0, \psi_0 \in L^\infty(\Omega)$, then

$$\|\varphi\|_{L^\infty(\Omega_T)} \leq c(1 + \|\varphi_0\|_{L^\infty(\Omega)}) \quad \text{and} \quad \|\psi\|_{L^\infty(\Omega_T)} \leq c(1 + \|\psi_0\|_{L^\infty(\Omega)}), \qquad (4)$$

where $c > 0$ is a constant depending on the time interval $(0, T)$ and on the problem functions.

Remark 2.2. As a byproduct of this result we see that $\mathcal{H}^+$ is invariant by the flow and coincides with the biologically relevant region.

3. **Directional derivatives of the control to state map.** Henceforth, let $z_0 = (u_0, \varphi_0, \psi_0) \in \mathcal{H}^+ \cap [L^\infty(\Omega)]^3$ be fixed: we will now study the mapping

$$\begin{aligned} G : \mathcal{U} \doteq L^\infty(\Omega_T) \times L^\infty(\Omega_T) &\to \mathcal{H}^+\\ (\mathsf{v}, \mathsf{s}) &\mapsto z = (u, \varphi, \psi) \end{aligned}$$

where $z = z(\mathsf{v}, \mathsf{s}) = (u, \varphi, \psi)$ is the unique weak solution to (1) corresponding to the fixed data and therapies. Indeed, since (v, s) satisfies (H5), Theorem 2.1 applies ensuring the existence of $z = z(\mathsf{v}, \mathsf{s}) = (u, \varphi, \psi)$ where, in particular, $0 \leq u \leq 1$ and $\varphi, \psi \geq 0$ a.e. in Ω_T.

Thus G is well defined and is Lipschitz continuous by (3), provided that we endow $L^\infty(\Omega_T)$ with the topology of $L^2(\Omega_T)$. Our next aim is proving that it admits certain directional derivatives in proper directions at any point in $\mathcal{U}$. With this

purpose, having fixed $(\mathsf{v}^*, \mathsf{s}^*) \in \mathcal{U}$, we linearize our system at the corresponding state $z^* = (u^*, \varphi^*, \psi^*) = G(\mathsf{v}^*, \mathsf{s}^*)$. The linearized problem can be stated more easily if, taking advantage of the invariance of $\mathcal{H}^+$, we exploit the functions $\kappa(r) = -r(1-r)$ for $r \in [0,1]$ and $f_\lambda(s) = \dfrac{s}{\lambda + s}$ for $s \geq 0$, where $\lambda > 0$. Indeed, with these choices the original problem reads as

$$\begin{cases} \partial_t u - \operatorname{div}(D\nabla u) = [p(\mathsf{s})\mathsf{v} - a(\varphi+\psi)]\,\kappa(u) - u g(\varphi+\psi), & \text{in } \Omega_T \\ \partial_t \varphi - \Delta\varphi + [\kappa_0 + \mathrm{k}(\mathsf{s})u][f_K(\varphi) - f_{K'}(\psi)] = [\beta_0 + \mathrm{b}(\mathsf{s})u]J, & \text{in } \Omega_T, \\ \partial_t \psi - \Delta\psi + [\kappa_0 + \mathrm{k}(\mathsf{s})u][f_{K'}(\psi) - f_K(\varphi)] & \\ \quad = [F_0 + \mathrm{F}(\mathsf{s})u]\,[L(u) - \psi]\,, & \text{in } \Omega_T, \\ D\nabla u \cdot \mathbf{n} = \partial_{\mathbf{n}}\varphi = \partial_{\mathbf{n}}\psi = 0, & \text{on } \Sigma_T, \\ u(0) = u_0, \quad \varphi(0) = \varphi_0, \quad \psi(0) = \psi_0, & \text{in } \Omega. \end{cases} \tag{5}$$

Therefore, for fixed $(\mathsf{v}, \mathsf{s}) \in \mathcal{U}$, the problem linearized at z^* turns into

$$\begin{cases} \partial_t Y - \operatorname{div}(D\nabla Y) - AY - B\Phi - C\Psi = \Lambda\mathsf{v} + \Pi\mathsf{s} & \text{in } \Omega_T \\ \partial_t \Phi - \Delta\Phi - EY - Q\Phi - G\Psi = \Xi\mathsf{s} & \text{in } \Omega_T \\ \partial_t \Psi - \Delta\Psi + F_0\Psi - RY - H\Phi - M\Psi = N\mathsf{s} & \text{in } \Omega_T \\ D\nabla Y \cdot \mathbf{n} = \partial_{\mathbf{n}}\Phi = \partial_{\mathbf{n}}\Psi = 0 & \text{in } \Sigma_T \\ Y(0) = \Phi(0) = \Psi(0) = 0 & \text{in } \Omega \end{cases} \tag{6}$$

being the coefficients

$$\begin{aligned} A &= [p(\mathsf{s}^*)\mathsf{v}^* - a(\varphi^*+\psi^*)]\kappa'(u^*) - g(\varphi^*+\psi^*) & Q &= -H = -[\kappa_0 + \mathrm{k}(\mathsf{s}^*)u^*]f'_K(\varphi^*) \\ B &= -a'(\varphi^*+\psi^*)\kappa(u^*) - u^* g'(\varphi^*+\psi^*) & G &= [\kappa_0 + \mathrm{k}(\mathsf{s}^*)u^*]f'_{K'}(\psi^*) \\ C &= -a'(\varphi^*+\psi^*)\kappa(u^*) - u^* g'(\varphi^*+\psi^*) & \Lambda &= p(\mathsf{s}^*)\kappa(u^*) \\ E &= \mathrm{k}(\mathsf{s}^*)[f_{K'}(\psi^*) - f_K(\varphi^*)] + \mathrm{b}(\mathsf{s}^*)J & \Pi &= p'(\mathsf{s}^*)\mathsf{v}^*\kappa(u^*) \end{aligned}$$

$$\begin{aligned} R &= \mathrm{k}(\mathsf{s}^*)[f_K(\varphi^*) - f_{K'}(\psi^*)] + \mathrm{F}(\mathsf{s}^*)(L(u^*) - \psi^*) + [F_0 + \mathrm{F}(\mathsf{s}^*)u^*]L'(u^*) \\ M &= -[\kappa_0 + \mathrm{k}(\mathsf{s}^*)u^*]f'_{K'}(\psi^*) - \mathrm{F}(\mathsf{s}^*)u^* \\ N &= [\mathrm{k}'(\mathsf{s}^*)(f_K(\varphi^*) - f_{K'}(\psi^*)) + \mathrm{F}'(\mathsf{s}^*)(L(u^*) - \psi^*)]u^* \\ \Xi &= [\mathrm{k}'(\mathsf{s}^*)(f_{K'}(\psi^*) - f_K(\varphi^*)) + \mathrm{b}'(\mathsf{s}^*)J]u^*. \end{aligned}$$

Notice that, by the invariance of $\mathcal{H}^+$ and (4), the coefficients and the righthand side in (6) are in $L^\infty(\Omega_T)$, thus classical results on linear parabolic systems (see, e.g., [18, Theorem 1.1, Chapter IV]) yield the existence of a unique strong solution $Z = (Y, \Phi, \Psi) \in \mathcal{X} = C([0,T], \mathcal{V}) \cap L^2(0,T; [H^2(\Omega)]^3) \cap H^1(0,T; \mathcal{H})$ to (6) satisfying

$$\|Z\|^2_{\mathcal{X}} \leq c(\|\mathsf{v}\|^2_{L^2(\Omega_T)} + \|\mathsf{s}\|^2_{L^2(\Omega_T)}). \tag{7}$$

Now the existence of the directional derivative of the control to state map is stated in the next

Theorem 3.1. *Assuming (H1)–(H4) and (H6)–(H9), let $z_0 \in \mathcal{H}^+ \cap [L^\infty(\Omega)]^3$ be fixed and $(\mathsf{v}^*, \mathsf{s}^*) \in \mathcal{U}$ be a control with corresponding state $z^* = (u^*, \varphi^*, \psi^*)$. For*

any $(\bar{\mathsf{v}},\bar{\mathsf{s}}) \in \mathcal{U}$ *and* $\mu \in (0,1)$*, let* $(\mathsf{v}^\mu,\mathsf{s}^\mu) = (\mathsf{v}^* + \mu(\bar{\mathsf{v}} - \mathsf{v}^*), \mathsf{s}^* + \mu(\bar{\mathsf{s}} - \mathsf{s}^*))$ *with corresponding state* $z^\mu = (u^\mu, \varphi^\mu, \psi^\mu)$*. Then*

$$\lim_{\mu\to 0^+} \frac{z^\mu - z^*}{\mu} = Z \quad in \quad C([0,T];\mathcal{H}) \cap L^2(0,T;\mathcal{V}),$$

being $Z = (Y,\Phi,\Psi)$ *the solution to* (6)*.*

Proof. A direct application of (3) entails

$$z^\mu - z^* \to (0,0,0) \quad \text{in} \quad C([0,T];\mathcal{H}) \cap L^2(0,T;\mathcal{V}), \tag{8}$$

owing to the convergence $(\mathsf{v}^\mu,\mathsf{s}^\mu) \to (\mathsf{v}^*,\mathsf{s}^*)$ in $[L^2(\Omega_T)]^2$ as $\mu \to 0^+$.

We can now accomplish our purpose, taking advantage of the triplet

$$Y^\mu = \frac{u^\mu - u^*}{\mu} - Y, \quad \Phi^\mu = \frac{\varphi^\mu - \varphi^*}{\mu} - \Phi, \quad \Psi^\mu = \frac{\psi^\mu - \psi^*}{\mu} - \Psi,$$

where (Y,Φ,Ψ) solves (6). Indeed, the thesis can be rephrased as

$$\lim_{\mu\to 0^+} (Y^\mu,\Phi^\mu,\Psi^\mu) = (0,0,0) \quad \text{in} \quad C([0,T];\mathcal{H}) \cap L^2(0,T;\mathcal{V}).$$

Denoting by $Z^\mu = (Y^\mu,\Phi^\mu,\Psi^\mu)$ and $Z = (Y,\Phi,\Psi)$, long but easy computations reported in Appendix allow to prove that Z^μ solves

$$\partial_t Z^\mu + \mathcal{A}Z^\mu = \mathbb{A}Z^\mu + \mathbb{B}Z + \mathbb{C}, \tag{9}$$

supplemented with null initial and Neumann boundary conditions. Here $\mathcal{A}$ is the differential operator

$$\mathcal{A}Z^\mu = \begin{pmatrix} -\mathrm{div}[D\nabla Y^\mu] \\ -\Delta\Phi^\mu \\ -\Delta\Psi^\mu + F_0\Psi^\mu \end{pmatrix}$$

while $\mathbb{A},\mathbb{B},\mathbb{C}$ correspond to the matrices

$$\mathbb{A} = \begin{pmatrix} A_1 & A_2 & A_3 \\ A_4 & A_5 & A_6 \\ A_7 & A_8 & A_9 \end{pmatrix} \qquad \mathbb{B} = \begin{pmatrix} B_1 & B_2 & B_3 \\ B_4 & B_5 & B_6 \\ B_7 & B_8 & B_9 \end{pmatrix} \qquad \mathbb{C} = \begin{pmatrix} C_0\mathsf{v} + C_1\mathsf{s} \\ C_2\mathsf{s} \\ C_3\mathsf{s} \end{pmatrix}.$$

The precise coefficients are explicitly written in the Appendix where we also see that the entries $A_k, B_k, C_j \in L^\infty(\Omega_T)$ with

$$\|A_k\|_{L^\infty(\Omega_T)} \le C \quad \text{while} \quad \lim_{\mu\to 0^+} \|B_k\|_{L^2(0,T;H)} = 0, \quad k = 1,\dots,9, \tag{10}$$

owing to the continuity of the nonlinearities and to the convergences in the subsequent (19). In particular,

$$\lim_{\mu\to 0^+} \|\mathbb{B}\|_{L^2(0,T;H)} = 0,$$

where $\|\mathbb{B}\|^2_{L^2(0,T;H)} = \sum_{i=1}^9 \|B_i\|^2_{L^2(0,T;H)}$. Having explicited in the Appendix the coefficients C_j's and recalling that $\mathsf{v},\mathsf{s} \in L^\infty(\Omega_T)$, it is readily seen that

$$\lim_{\mu\to 0^+} \|\mathbb{C}\|_{L^2(0,T;\mathcal{H})} = 0. \tag{11}$$

Since, owing to (H4),

$$(\mathcal{A}Z^\mu, Z^\mu) \ge d\|\nabla Y^\mu\|^2 + \|\nabla\Phi^\mu\|^2 + \|\nabla\Psi^\mu\|^2 \ge \omega\|\nabla Z^\mu\|^2$$

for $\omega = \min\{d,1\}$, then the scalar product in $\mathcal{H}$ of system (9) by Z^μ, followed by an integration in $(0,t)$, lead to

$$\frac{1}{2}\|Z^\mu(t)\|^2 + \omega\int_0^t \|\nabla Z^\mu\|^2\,ds$$

$$\le \int_0^t \int_\Omega [|A_1| + |A_5| + |A_9|]|Z^\mu|^2 \, dxds + \int_0^t ((A_2 + A_4)Y^\mu, \Phi^\mu) \, ds + \int_0^t (\mathbb{C}, Z^\mu) \, ds$$
$$+ \int_0^t ((A_6 + A_8)\Phi^\mu, \Psi^\mu) \, ds + \int_0^t ((A_3 + A_7)Y^\mu, \Psi^\mu) \, ds + \int_0^t (\mathbb{B}Z, Z^\mu) \, ds,$$

due to $\|Z^\mu(0)\| = 0$. The first four integrals on the righthand side are easily controlled thanks to (10) as

$$\int_0^t \int_\Omega [|A_1| + |A_5| + |A_9|]|Z^\mu|^2 \, dxds + \int_0^t ((A_2 + A_4)Y^\mu, \Phi^\mu) \, ds$$
$$+ \int_0^t ((A_6 + A_8)\Phi^\mu, \Psi^\mu) \, ds + \int_0^t ((A_3 + A_7)Y^\mu, \Psi^\mu) \, ds$$
$$\le c \int_0^t \|Z^\mu\|_{\mathcal{H}}^2 \, ds,$$

while, on account of $\|Z\|_{L^\infty(0,T;\mathcal{V})} \le c$ by (7), we obtain

$$\int_0^t (\mathbb{B}Z, Z^\mu) \, ds + \int_0^t (\mathbb{C}, Z^\mu) \, ds$$
$$\le \int_0^t (\|\mathbb{B}\|\|Z\|_{\mathcal{V}}\|Z^\mu\|_{\mathcal{V}} + \|\mathbb{C}\|\|Z^\mu\|) \, ds$$
$$\le \frac{\omega}{2} \int_0^t \|\nabla Z^\mu\|_{\mathcal{H}}^2 \, ds + c \int_0^t \|Z^\mu\|_{\mathcal{H}}^2 \, ds + c \left(\|\mathbb{B}\|_{L^2(0,T;H)}^2 + \|\mathbb{C}\|_{L^2(0,T;\mathcal{H})}^2 \right).$$

Collecting these estimates we are lead to

$$\|Z^\mu(t)\|_{\mathcal{H}}^2 + \omega \int_0^t \|\nabla Z^\mu\|_{\mathcal{H}}^2 \, ds$$
$$\le c \int_0^t \|Z^\mu\|_{\mathcal{H}}^2 \, ds + c \left(\|\mathbb{B}\|_{L^2(0,T;H)}^2 + \|\mathbb{C}\|_{L^2(0,T;\mathcal{H})}^2 \right),$$

so that, by Gronwall's Lemma, it follows

$$\|Z^\mu(t)\|_{\mathcal{H}}^2 + \omega \int_0^t \|\nabla Z^\mu\|_{\mathcal{H}}^2 \, ds \le c \left(\|\mathbb{B}\|_{L^2(0,T;H)}^2 + \|\mathbb{C}\|_{L^2(0,T;\mathcal{H})}^2 \right) e^{cT}.$$

Passing to the limit as $\mu \to 0^+$, we conclude on account of (10) and (11). □

4. **The control problem.** Our final task is to establish the existence and devise a necessary condition for a control $(\mathsf{v}^*, \mathsf{s}^*)$ to be optimal; this allows to numerically determine an optimal therapeutic strategy in terms of the cytotoxic and anti-angiogenic treatments. The functional to minimize is

$$\mathcal{J}(u, \varphi, \psi, \mathsf{v}, \mathsf{s})$$
$$= \frac{k_1}{2} \int_{\Omega_T} [u(x,t) - u_Q(x,t)]^2 \, dxdt + \frac{k_2}{2} \int_\Omega [u(x,T) - u_\Omega(x)]^2 \, dx + k_3 \int_\Omega u(x,T) \, dx$$
$$+ \frac{k_4}{2} \int_{\Omega_T} [\varphi(x,t) + \psi(x,t) - \ell_Q(x,t)]^2 \, dxdt$$
$$+ \frac{k_5}{2} \int_\Omega [\varphi(x,T) + \psi(x,T) - \ell_\Omega(x)]^2 \, dx$$
$$+ \frac{k_6}{2} \int_{\Omega_T} \mathsf{v}^2(x,t) \, dxdt + \frac{k_7}{2} \int_{\Omega_T} \mathsf{s}^2(x,t) \, dxdt.$$

for any $(u,\varphi,\psi) \in C([0,T];\mathcal{H})$ and any $(\mathsf{v},\mathsf{s}) \in L^2(0,T;H^2)$. Here $k_i \geq 0$ are constants while the functions

$$u_Q, \ell_Q \in L^2(\Omega_T) \quad \text{and} \quad u_\Omega, \ell_\Omega \in L^2(\Omega) \tag{12}$$

represent suitable targets. Actually, we are interested in minimizing a restriction of $\mathcal{J}$, in the sense that we fix $z_0 \in \mathcal{H}^+ \cap [L^\infty(\Omega)]^3$, then (u,φ,ψ) is the state, that is, the weak solution to (1) with z_0 as initial datum, corresponding to the pair (v,s) that in turn varies in the set of the admissible controls

$$\mathcal{U}_{\rm ad} = \{(\mathsf{v},\mathsf{s}) \in [L^2(\Omega_T)]^2 : \quad 0 \leq \mathsf{v} \leq V_{\max}, \quad 0 \leq \mathsf{s} \leq S_{\max}\},$$

being $V_{\max} > 0$ and $S_{\max} > 0$ fixed. Since the assumptions of Theorem 2.1 hold true, for any fixed initial datum $z_0 \in \mathcal{H}^+ \cap [L^\infty(\Omega)]^3$, the control to state map is well-defined and Lipschitz continuous with respect to the $[L^2(\Omega_T)]^2-$norm. Besides, it admits directional derivatives in any direction at any point by Theorem 3.1. Denoting the state corresponding to the control $(\mathsf{v},\mathsf{s}) \in \mathcal{U}_{ad}$ as $z = (u,\varphi,\psi) = z(\mathsf{v},\mathsf{s})$, our purpose is minimizing the functional $\mathsf{J}(\mathsf{v},\mathsf{s}) = \mathcal{J}(z(\mathsf{v},\mathsf{s}),\mathsf{v},\mathsf{s})$ in $\mathcal{U}_{ad}$. In order to do so, we first establish the existence of an optimal control.

Lemma 4.1. *Provided that (H1)–(H4), (H6)–(H9) and (12) hold true, then for any initial datum $(u_0,\varphi_0,\psi_0) \in \mathcal{H}^+ \cap [L^\infty(\Omega)]^3$ there exists at least an optimal control $(\mathsf{v}^*,\mathsf{s}^*) \in \mathcal{U}_{ad}$, that is,*

$$\mathsf{J}(\mathsf{v}^*,\mathsf{s}^*) = \min_{(\mathsf{v},\mathsf{s})\in\mathcal{U}_{ad}} \mathsf{J}(\mathsf{v},\mathsf{s}).$$

The proof of this result is as in [11, Theorem 6.1] (see also [10]) but we write it for the reader's convenience:

Proof. Indeed, since $\mathsf{J} \geq 0$, it is immediate to see that $\inf_{(\mathsf{v},\mathsf{s})\in\mathcal{U}_{ad}} \mathsf{J}(\mathsf{v},\mathsf{s}) = \delta \geq 0$. We can consider then a minimizing sequence $(\mathsf{v}_n,\mathsf{s}_n) \in \mathcal{U}_{ad}$ such that

$$\delta \leq \mathsf{J}(\mathsf{v}_n,\mathsf{s}_n) \leq \delta + \frac{1}{n}, \quad \forall n \in \mathbb{N},$$

and, according to Theorem 2.1, the corresponding state (u_n,φ_n,ψ_n): this, in particular is uniformly bounded in $L^2(0,T;\mathcal{V}) \cap C([0,T];\mathcal{H}) \cap H^1(0,T;\mathcal{V}')$ with $0 \leq u_n \leq 1$ a.e. in Ω_T and $\varphi_n, \psi_n \geq 0$ a.e. in Ω_T satisfy (4). By the boundedness of $\mathcal{U}_{ad}$ and (2), we can select subsequences (that we still denote as) $(\mathsf{v}_n,\mathsf{s}_n)$ and (u_n,φ_n,ψ_n) such that

$$(\mathsf{v}_n,\mathsf{s}_n) \to (\mathsf{v}^*,\mathsf{s}^*) \quad \text{weakly star in } L^\infty(\Omega_T) \times L^\infty(\Omega_T),$$

$$(u_n,\varphi_n,\psi_n) \to (u^*,\varphi^*,\psi^*) \text{ weakly in } H^1(0,T;\mathcal{V}') \cap L^2(0,T;\mathcal{V}) \text{ and weakly star in } L^\infty(\Omega_T).$$

It is worth noticing that so far no relation connects $(\mathsf{v}^*,\mathsf{s}^*)$ and (u^*,φ^*,ψ^*). Our aim will be to prove that $(u^*,\varphi^*,\psi^*) = G(\mathsf{v}^*,\mathsf{s}^*)$, namely, that (u^*,φ^*,ψ^*) is the state corresponding to the control, and that $\mathsf{J}(\mathsf{v}^*,\mathsf{s}^*) = \delta$. First of all, by compactness,

$$(u_n,\varphi_n,\psi_n) \to (u^*,\varphi^*,\psi^*) \quad \text{strongly in } L^2(0,T;\mathcal{H}), \tag{13}$$

and, owing to the Ascoli-Arzelá Theorem,

$$(u_n(t),\varphi_n(t),\psi_n(t)) \to (u^*(t),\varphi^*(t),\psi^*(t)) \quad \text{strongly in } \mathcal{V}', \text{ uniformly in } t \in [0,T]. \tag{14}$$

Therefore, it follows that $(u^*(0), \varphi^*(0), \psi^*(0)) = (u_0, \varphi_0, \psi_0)$. Besides, $(u^*, \varphi^*, \psi^*) \in \mathcal{H}^+$ and that φ^* and ψ^* satisfy (4). Furthermore, due to the boundedness and Lipschitz continuity of all the involved nonlinear functions, these convergences allow to pass to the limit in the problem solved by (u_n, φ_n, ψ_n), proving that (u^*, φ^*, ψ^*) solves the initial boundary value problem correspondig to $(\mathsf{v}^*, \mathsf{s}^*)$, that is, $(u^*, \varphi^*, \psi^*) = G(\mathsf{v}^*, \mathsf{s}^*)$.

To accomplish our second task, we decompose the functional J in three parts, namely,

$$\mathsf{J} = \mathsf{J}_1 + \mathsf{J}_2 + \mathsf{J}_3,$$

where

$$\begin{aligned}
\mathsf{J}_1(\mathsf{v}, \mathsf{s}) &= \frac{k_1}{2} \int_{\Omega_T} [u(x,t) - u_Q]^2 dxdt + \frac{k_4}{2} \int_{\Omega_T} [\varphi(x,t) + \psi(x,t) - \ell_Q]^2 dxdt, \\
\mathsf{J}_2(\mathsf{v}, \mathsf{s}) &= k_3 \int_{\Omega} u(x,T) dx, \\
\mathsf{J}_3(\mathsf{v}, \mathsf{s}) &= \frac{k_2}{2} \int_{\Omega} [u(x,T) - u_\Omega]^2 dx + \frac{k_5}{2} \int_{\Omega} [\varphi(x,T) + \psi(x,T) - \ell_\Omega]^2 dx \\
&\quad + \frac{k_6}{2} \int_{\Omega_T} \mathsf{v}^2(x,t) dxdt + \frac{k_7}{2} \int_{\Omega_T} \mathsf{s}^2(x,t) dxdt.
\end{aligned}$$

Now, convergence (13) immediately gives

$$\lim_{n\to\infty} \mathsf{J}_1(\mathsf{v}_n, \mathsf{s}_n) = \mathsf{J}_1(\mathsf{v}^*, \mathsf{s}^*).$$

By the uniform boundedness of $\|u_n(T)\|$ following from (2), we infer that, up to a subsequence,

$$u_n(T) \to u^*(T) \quad \text{weakly in} \quad H$$

so that

$$\lim_{n\to\infty} \mathsf{J}_2(\mathsf{v}_n, \mathsf{s}_n) = \mathsf{J}_2(\mathsf{v}^*, \mathsf{s}^*).$$

The last functional J_3 is weakly lower semicontinuous thus

$$\mathsf{J}_3(\mathsf{v}^*, \mathsf{s}^*) \le \liminf_{n\to\infty} \mathsf{J}_3(\mathsf{v}_n, \mathsf{s}_n).$$

Collecting all our computations, we conclude

$$\delta \le \mathsf{J}(\mathsf{v}^*, \mathsf{s}^*) \le \liminf_{n\to\infty} \mathsf{J}(\mathsf{v}_n, \mathsf{s}_n) = \delta,$$

showing that indeed J realizes its minimum value at $(\mathsf{v}^*, \mathsf{s}^*)$. □

We are now in the position to numerically determine an optimal control if we can detect a necessary optimality condition in a geometrically meaningful form (see e.g. [25]). To accomplish our task, we take advantage of Theorem 3.1 and of the solution to an additional linear problem. Indeed, we consider the adjoint system to

(6), in the unknowns (y, ϕ, χ), reading as

$$\begin{cases} -\partial_t y - \operatorname{div}(D\nabla y) = Ay + E\phi + R\chi + k_1(u^* - u_Q) & \text{in } \Omega_T \\ -\partial_t \phi - \Delta\phi = By + Q\phi + H\chi + k_4(\varphi^* + \psi^* - \ell_Q) & \text{in } \Omega_T \\ -\partial_t \chi - \Delta\chi + F_0\chi = Cy + G\phi + M\chi + k_4(\varphi^* + \psi^* - \ell_Q) & \text{in } \Omega_T \\ D\nabla y \cdot \mathbf{n} = \partial_{\mathbf{n}}\phi = \partial_{\mathbf{n}}\chi = 0 & \text{in } \Sigma_T \\ y(T) = k_2[u^*(T) - u_\Omega] + k_3, & \text{in } \Omega, \\ \phi(T) = k_5[\varphi^*(T) + \psi^*(T) - \ell_\Omega], & \text{in } \Omega, \\ \chi(T) = k_5[\varphi^*(T) + \psi^*(T) - \ell_\Omega] & \text{in } \Omega, \end{cases} \tag{15}$$

where k_i are the constants appearing in the functional $\mathcal{J}$ while the coefficients are defined as in (6). Applying [11, Theorema 7.1](based on [16, Theorem 7.1, p. 181]), we see that this problem admits a unique weak solution $(y, \phi, \chi) \in L^2(0, t; \mathcal{V}) \cap C([0, T]; \mathcal{H}) \cap H^1(0, T; \mathcal{V}')$, that allows to explicit the first order optimality condition as

Lemma 4.2. *Provided that (H1)–(H4), (H6)–(H9) and (12) hold true, if $(\mathsf{v}^*, \mathsf{s}^*) \in \mathcal{U}_{ad}$ is an optimal control and (u^*, φ^*, ψ^*) is the corresponding optimal state, then*

$$\mathsf{v}^* = \mathbb{P}_{K_1}\left(-\frac{\Lambda y}{k_6}\right) \qquad \text{and} \qquad \mathsf{s}^* = \mathbb{P}_{K_2}\left(-\frac{\Pi y + \Xi\phi + N\chi}{k_7}\right)$$

where (y, ϕ, χ) is the solution to (15) and $\mathbb{P}_{K_i}$ stands for the projection on K_i $(i = 1, 2)$ defined as

$$K_1 = \{\mathsf{v} \in L^2(\Omega_T) : \quad 0 \le \mathsf{v} \le V_{\max}\} \quad \text{and} \quad K_2 = \{\mathsf{s} \in L^2(\Omega_T) : \quad 0 \le \mathsf{s} \le S_{\max}\}.$$

Proof. Assume that $(\mathsf{v}^*, \mathsf{s}^*) \in \mathcal{U}_{ad}$ is an optimal control and (u^*, φ^*, ψ^*) is the corresponding optimal state. For any fixed $(\bar{\mathsf{v}}, \bar{\mathsf{s}}) \in \mathcal{U}_{ad}$ and any $\mu \in (0, 1)$, we define $(\mathsf{v}^\mu, \mathsf{s}^\mu) = (\mathsf{v}^* + \mu(\bar{\mathsf{v}} - \mathsf{v}^*), \mathsf{s}^* + \mu(\bar{\mathsf{s}} - \mathsf{s}^*))$. Since $(\mathsf{v}^\mu, \mathsf{s}^\mu) \in \mathcal{U}_{ad}$ by the convexity of this set, we can consider the corresponding state $(u^\mu, \varphi^\mu, \psi^\mu)$ and observe that

$$\frac{\mathsf{J}(\mathsf{v}^\mu, \mathsf{s}^\mu) - \mathsf{J}(\mathsf{v}^*, \mathsf{s}^*)}{\mu} \ge 0, \quad \forall \mu \in (0, 1).$$

By Theorem 3.1, we can pass to the limit as $\mu \to 0^+$, proving that the directional derivative of J in $(\mathsf{v}^*, \mathsf{s}^*)$ in the direction $(\bar{\mathsf{v}} - \mathsf{v}^*, \bar{\mathsf{s}} - \mathsf{s}^*)$ is nonnegative and reads as

$$\begin{aligned} &\Big\{k_1 \int_{\Omega_T} (u^* - u_Q) Y dxdt + k_2 \int_\Omega (u^*(T) - u_\Omega) Y(T) dx + k_3 \int_\Omega Y(x, T) dx \\ &+ k_4 \int_{\Omega_T} (\varphi^*(x, t) + \psi^*(x, t) - \ell_Q)(\Phi + \Psi) dxdt \\ &+ k_5 \int_\Omega [\varphi^*(T) + \psi^*(T) - \ell_\Omega](\Phi(T) + \Psi(T)) dx\Big\} \\ &+ k_6 \int_{\Omega_T} \mathsf{v}^*(\bar{\mathsf{v}} - \mathsf{v}^*) dxdt + k_7 \int_{\Omega_T} \mathsf{s}^*(\bar{\mathsf{s}} - \mathsf{s}^*) dxdt \ge 0, \end{aligned} \tag{16}$$

On the other hand, taking advantage of the adjoint problem, we see that

$$\begin{aligned} &k_1 \int_{\Omega_T} (u^* - u_Q) Y dxdt + k_2 \int_\Omega (u^*(T) - u_\Omega) Y(T) dx + k_3 \int_\Omega Y(x, T) dx \\ &+ k_4 \int_{\Omega_T} (\varphi^*(x, t) + \psi^*(x, t) - \ell_Q)(\Phi + \Psi) dxdt \end{aligned}$$

$$+ k_5 \int_\Omega [\varphi^*(T) + \psi^*(T) - \ell_\Omega](\Phi(T) + \Psi(T))dx$$
$$= \int_{\Omega_T} [\Lambda(\bar{\mathsf{v}} - \mathsf{v}^*)y + (\bar{\mathsf{s}} - \mathsf{s}^*)(\Pi y + \Xi\phi + N\chi)]dxdt.$$

To prove this, just multiply the equations in (15) by Y, Φ and Ψ, respectively. Replacing this last equality in (16), we obtain the optimality condition as

$$\int_{\Omega_T} [\Lambda(\bar{\mathsf{v}} - \mathsf{v}^*)y + (\bar{\mathsf{s}} - \mathsf{s}^*)(\Pi y + \Xi\phi + N\chi)]dxdt$$
$$+ k_6 \int_{\Omega_T} \mathsf{v}^*(\bar{\mathsf{v}} - \mathsf{v}^*)dxdt + k_7 \int_{\Omega_T} \mathsf{s}^*(\bar{\mathsf{s}} - \mathsf{s}^*)dxdt \geq 0,$$

so that the elementary theory of Hilbert spaces leads to the desired expression. □

Let us conclude our analysis by expressing the optimal control in the easiest possible form, recalling that the projection of $v \in L^2(\Omega_T)$ into

$$K = \{x \in L^2(\Omega_T) : 0 \leq x \leq b \text{ a.e. in } \Omega_T\}$$

is

$$\mathbb{P}_K(v) = \begin{cases} 0 & \text{if } v < 0, \\ v & \text{if } 0 \leq v \leq b, \\ b & \text{if } v > b. \end{cases}$$

As a result, the optimal control $(\mathsf{v}^*, \mathsf{s}^*)$ is characterized as

$$\mathsf{v}^* = \begin{cases} 0, & \text{if} \quad -\Lambda y < 0, \\ -\dfrac{1}{k_6}\Lambda y, & \text{if} \quad 0 \leq -\dfrac{1}{k_6}\Lambda y \leq V_{\max}, \\ V_{\max}, & \text{if} \quad -\dfrac{1}{k_6}\Lambda y > V_{\max}, \end{cases}$$

and

$$\mathsf{s}^* = \begin{cases} 0, & \text{if} \quad -(\Pi y + \Xi\phi + N\chi) < 0, \\ -\dfrac{1}{k_7}(\Pi y + \Xi\phi + N\chi), & \text{if} \quad 0 \leq -\frac{1}{k_7}(\Pi y + \Xi\phi + N\chi) \leq S_{\max}, \\ S_{\max}, & \text{if} \quad -\dfrac{1}{k_7}(\Pi y + \Xi\phi + N\chi) > S_{\max}. \end{cases}$$

5. Numerical simulations.

5.1. **A simplified model.** For the sake of simplicity, we fixed in the previous sections the carrying capacity γ (maximum number of cells that can fit $1\,mm^3$ of tissue) to one, yielding that the tumor concentration remains in the interval $[0, \gamma] = [0, 1]$. Now, as far as the numerical simulations are concerned, we consider a more realistic carrying capacity, namely $\gamma = 10^6$ (see [13]).

We neglect the necrosis of the tumor, assuming that $g(\varphi + \psi) = 0$. Moreover in the following simulations, the antiangiogenic/antiepileptic treatment s is fixed and we only search for the optimal chemotherapy quantities required to achieve the desired reduction of the tumor. Therefore, in the cost functional $k_7 = 0$ and, since in practice we cannot target lactate concentrations with the sole chemotherapy treatment, $k_4 = k_5 = 0$ as well. Besides, we set $k_3 = 0$ and we normalize $p(\mathsf{s}) = 1$. Finally we assumed the arterial lactate L to depend on s as well: notice that the computations of the previous sections can be repeated without any difficulty.

Hence we transform our equations as follows :

$$\begin{cases} \partial_t u - \operatorname{div}(D\nabla u) = -[a(\varphi+\psi) - \mathsf{v}]\,\kappa(u), & \text{in } \Omega_T \\ \partial_t \varphi - \alpha\Delta\varphi + k(\frac{u}{\gamma},\mathsf{s})\left(\dfrac{\varphi}{K+\varphi} - \dfrac{\psi}{K'+\psi}\right) = \beta(\frac{u}{\gamma},\mathsf{s})J, & \text{in } \Omega_T, \\ \epsilon\partial_t\psi - \varrho\Delta\psi + k(\frac{u}{\gamma},\mathsf{s})\left(\dfrac{\psi}{K'+\psi} - \dfrac{\varphi}{K+\varphi}\right) & \\ = F(\frac{u}{\gamma},\mathsf{s})\left[L(\frac{u}{\gamma},\mathsf{s}) - \psi\right], & \text{in } \Omega_T, \\ D\nabla u\cdot\mathbf{n} = \partial_{\mathbf{n}}\varphi = \partial_{\mathbf{n}}\psi = 0, & \text{on } \Sigma_T, \\ u(0) = u_0, \quad \varphi(0) = \varphi_0, \quad \psi(0) = \psi_0, & \text{in } \Omega, \end{cases} \tag{17}$$

where $\kappa(u) = -u(1-\frac{u}{\gamma})$. According to the previous assumptions, we used the following reduced functional:

$$\begin{aligned} \mathcal{J}(u,\mathsf{v}) =& \frac{k_1}{2\gamma^2}\int_0^T\int_\Omega [u(x,t)-u_Q]^2 dx\,dt + \frac{k_2}{2\gamma^2}\int_\Omega [u(x,T)-u_\Omega]^2\,dx \\ &+ \frac{k_6}{2}\int_0^T \mathsf{v}^2(x,t)\,dt, \end{aligned}$$

and the corresponding adjoint problem:

$$\begin{cases} -\partial_t y - \operatorname{div}(D\nabla y) = Ay + E\phi + R\chi + k_1(u^* - u_Q) & \text{in } \Omega_T \\ -\partial_t\phi - \alpha\Delta\phi = By + Q\phi + H\chi & \text{in } \Omega_T \\ -\epsilon\partial_t\chi - \varrho\Delta\chi + F_0\chi = Cy + G\phi + M\chi & \text{in } \Omega_T \\ D\nabla y\cdot\mathbf{n} = \partial_{\mathbf{n}}\phi = \partial_{\mathbf{n}}\chi = 0 & \text{in } \Sigma_T \\ y(T) = \dfrac{k_2}{\gamma^2}[u^*(T) - u_\Omega], & \text{in } \Omega, \\ \phi(T) = 0, & \text{in } \Omega, \\ \chi(T) = 0 & \text{in } \Omega, \end{cases} \tag{18}$$

with

$$\begin{aligned} &A = [\mathsf{v}^* - a(\varphi^*+\psi^*)]\left(2\frac{u^*}{\gamma} - 1\right), && B = C = a'(\varphi^*+\psi^*)u^*\left(1-\frac{u^*}{\gamma}\right), \\ &E = \frac{\mathrm{k}(\mathsf{s})}{\gamma}[f_{K'}(\psi^*) - f_K(\varphi^*)] + \frac{\mathrm{b}(\mathsf{s})}{\gamma}J, && Q = -H = -k(\frac{u^*}{\gamma},\mathsf{s})f_K'(\varphi^*), \\ &G = k(\frac{u^*}{\gamma},\mathsf{s})f_{K'}'(\psi^*), && M = -k(\frac{u^*}{\gamma},\mathsf{s})f_{K'}'(\psi^*) - \mathrm{F}(\mathsf{s})\frac{u^*}{\gamma}, \end{aligned}$$

$$R = \frac{\mathrm{k}(\mathsf{s})}{\gamma}[f_K(\varphi^*) - f_{K'}(\psi^*)] + \frac{\mathrm{F}(\mathsf{s})}{\gamma}(L(\frac{u^*}{\gamma},\tilde{\mathsf{s}}) - \psi^*) + \frac{1}{\gamma}F(\frac{u^*}{\gamma},\mathsf{s})L'(\frac{u^*}{\gamma},\mathsf{s}).$$

Consequently the derivative of $\mathcal{J}(u(\mathsf{v}),\mathsf{v}) = \tilde{J}(\mathsf{v})$ reads:

$$d_{\mathsf{v}}\tilde{J}(\mathsf{v}^*) = k_6\mathsf{v}^* + \int_\Omega \kappa(u^*)y\,dx,$$

where y is the solution of the adjoint problem.

Algorithm 1 Descent optimization algorithm

Require: $n = 0$ and $\mathsf{v}^0 = 0$, $E = 1$

while $E > 10^{-8}$ **do**

Solve the state equation (17) with $\mathsf{v} = \mathsf{v}^n$ on $[0, T]$ and get u^n, φ^n, ψ^n

Evaluate the functional $\mathcal{J}(u^n, \mathsf{v}^n)$

Find (y^n, ϕ^n, χ^n) solution to the adjoint equation (18) with $u^* = u^n$, $\varphi^* = \varphi^n$, $\psi^* = \psi^n$ and $\mathsf{v}^* = \mathsf{v}^n$

Evaluate the direction of descent $d^n = d_{\mathsf{v}}\tilde{J}(u^n)$

Search the descent step σ^n (Armijo's rule, see [5])

Update the control parameter

$$\mathsf{v}^{n+1} = \mathsf{v}^n + \sigma_n d^n$$

Evaluate the error $E = \dfrac{|\mathcal{J}(u^{n+1}, \mathsf{v}^{n+1}) - \mathcal{J}(u^n, \mathsf{v}^n)|}{|\mathcal{J}(u^{n+1}, \mathsf{v}^{n+1})|}$

end while

5.2. **Choices of the parameters and protocols.** For the simulations presented below, Ω is an ellipse parametrized by $x = 6\cos\theta$, $y = 8\sin\theta$, $\theta \in [0, 2\pi]$ representing the part of the brain surrounding the tumor. We discretize the equations (17) in space with a P_1- finite element method and in time with an implicit Euler scheme. The mesh step and the time step are respectively taken as $h = 10^{-2}$ and $\delta t = 0.01$. Moreover we take :

$$D = \begin{pmatrix} 0.01 & 0 \\ 0 & 0.005 \end{pmatrix}, \quad a(\varphi + \psi) = \frac{1}{2}\left(0.1 + 1.2\arctan(\frac{\varphi + \psi}{2})\right)^2.$$

We also choose $\epsilon = 0.1$, $K = K' = 3.5$, $\alpha = 0.05$ et $\varrho = 0.02$. Concerning the functional parameters we choose $k_1 = 10^4$ (or $k_1 = 0$, see the discussion below), $k_2 = 10^4$ and $k_6 = 1$.

We follow two protocols for the therapies:

Swanson's protocol The chemotherapy cycle is 6 weeks, $\mathsf{v}(t) = v$ during 2 weeks when the chemotherapy is being administered, and $\mathsf{v}(t) = 0$ during the following 4 weeks. This protocol was introduced by Swanson et al. in [22] for patients suffering from low grade glioma. The antiangiogenic/antiepileptic treatment is administered concomitant with the chemotherapy.

The computations are performed up to 30 weeks, with 5 cycles of chemotherapy, the first cycle starting at $t = 0$.

Stupp's protocol The chemotherapy cycle is 4 weeks, $\mathsf{v}(t) = v$ during five days when the chemotherapy is being administered, and $\mathsf{v}(t) = 0$ till the end of the cycle. This protocol was introduced by Stupp et al. in [21] for patients suffering from high grade glioma. The antiangiogenic/antiepileptic treatment is administered concomitant with the chemotherapy.

The computations are performed up to 24 weeks, with 6 cycles of chemotherapy, the first cycle starting at $t = 0$.

In this section we simulate the evolutions of the tumors and lactate concentrations for two virtual patients suffering from glioma. We illustrate that the efficiency of the chemotherapy is related to the lactate concentrations in the patients' tumor cells; more specifically, the higher the lactates concentrations, the weaker the efficacy of chemotherapy. Hence the chemotherapy could be less dosed if the treatment strategy targets, at the same time, the tumor and the lactates.

5.3. **Patient 1.** We set :

$$k(\frac{u}{\gamma},\mathsf{s}) = \kappa_0 + 3\,(1-\mathsf{s})\frac{u}{\gamma}, \quad \beta(\frac{u}{\gamma},\mathsf{s}) = 1 + 18\,(1-\mathsf{s})\frac{u}{\gamma}, \quad F(\frac{u}{\gamma},\mathsf{s}) = F_0 + 1.5\,(1-\mathsf{s})\frac{u}{\gamma},$$

$$L(\frac{u}{\gamma}) = L_0 + 3\frac{u}{\gamma}, \quad \text{with } \kappa_0 = 0.1, \quad F_0 = 0.0272, \quad \text{and} \quad L_0 = 0.8,\ J = 0.0272.$$

Here, κ_0, F_0, L_0 stand for normal values (in healthy tissues) of the maximum transport rate through monocarboxylate transporters, the cerebral blood flow and the arterial concentration respectively. The tumor area is centered at $(0, 0)$ and is delimited by a circle of radius $r = 0.8$.

5.3.1. *Swanson's protocol.* In Figure 1, we take $v = 2$, $\mathsf{s} = 0.9$, $u_0(x, y) = 3\,.\,10^5$, $\varphi_0 = 1.2$ and $\psi_0 = 0.5$ ($\varphi_0 + \psi_0 = 1.7$) inside the tumor area and $u_0(x, y) = 0$, $\varphi_0 = 0.8$, $\psi_0 = 0.5$ ($\varphi_0 + \psi_0 = 1.3$) outside. We compare the evolution of the tumor cell densities and of the sum of the lactate concentrations at the point $(0, 0)$ in four different cases: no treatment during the 30 weeks, only a chemotherapy treatment, only an antiangiogenic/antiepileptic treatment, and the combination of chemotherapy and lactate targeting treatments. Our results seem consistent with current knowledge, namely, the antiangiogenic/antiepileptic treatment is not efficient by itself, but enhances the effects of the chemotherapy.

Now we set $\mathsf{s} = 0.9$ and search for the minimal amount of chemotherapy required for reducing the tumor cell density to $u_\Omega = u_Q = 40000$. We get $v^* = 5.72$ when the chemotherapy is the only treatment, and $v^* = 5.47$ when the chemotherapy is combined with an antiangiogenic/antiepileptic treatment. Figure 2 displays the evolution of the tumor (above) and the lactates (below), submitted to the optimal quantities of chemotherapy in both therapeutic strategies. We see that the trajectories of the tumor cell densities coincide, whereas the dosage of chemotherapy and the trajectories of the lactate concentrations are lower when the treatment combines a chemotherapy and an antiangiogenic/antiepileptic drug.

5.3.2. *Stupp's protocol.* We take $u_0(x, y) = 6\,.\,10^5$ inside the tumor area and $u_0(x, y) = 0$ outside. We assume high initial lactate levels, namely $\varphi_0 = 6$, $\psi_0 = 2$ ($\varphi_0 + \psi_0 = 8$) inside the tumor area and $\varphi_0 = 0.8$, $\psi_0 = 0.5$ ($\varphi_0 + \psi_0 = 1.3$) outside. Moreover we choose $u_\Omega = u_Q = 10^5$ and $\mathsf{s} = 0$ (no antiangiogenic/antiepileptic therapy). The computations lead to $v^*(= v^*_{high}) = 17.41$. In the upper part of Figure 3, we show the evolution, with respect to time, of the tumor cells densities at the point (0,0) when the tumor is treated with the optimal amount of chemotherapy. In the lower part of Figure 3, we use in the optimization algorithm two different functionals $\mathcal{J}(u, \mathsf{v})$ (in the first one $k_1 = 0$, in the second one $k_1 = 10^4$) and compare the two convergences of the algorithms to the optimal chemotherapy. We can see that both functionals lead to the same optimal value, namely $v^* = 17.41$. Anyway the algorithm converges faster (with respect to the number of iterations) when $k_1 \neq 0$.

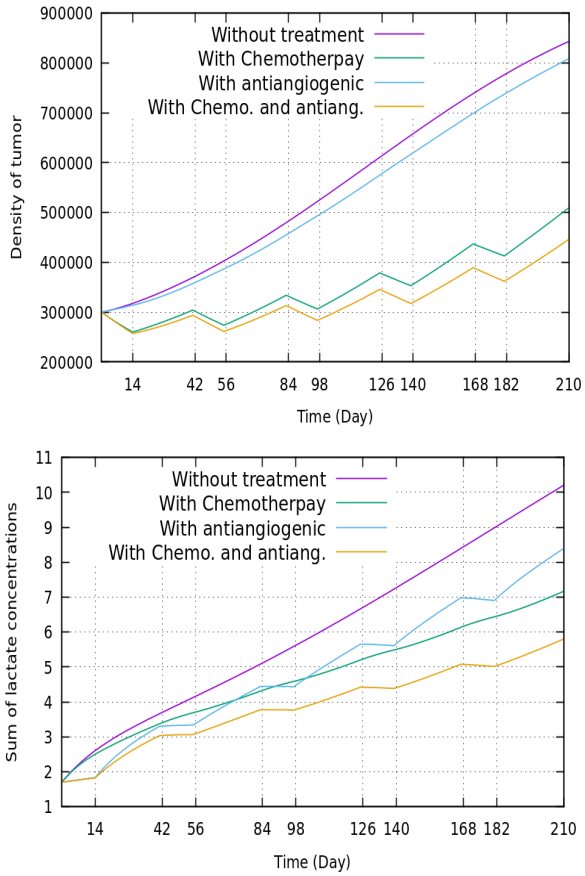

FIGURE 1. Patient 1, $v = 2$, Evolution of the tumor cell density (above) and the sum of lactate concentrations (below) with respect to time at the center of the tumor

In the upper part of Figure 4, the computations are performed with the same initial conditions and parameters as in Figure 3, except that the lactate concentration level is taken lower inside the tumor area, namely $\varphi_0 = 3$, $\psi_0 = 1$. This time we obtain $v^*(= v^*_{low}) = 16.1$, which validates the fact that the chemotherapy optimal dosage is smaller than it was in the case of high lactates. In the lower part of Figure 4, we compare the evolution of the tumor, in case of the high lactate levels of Figure 3 ($\varphi_0 + \psi_0 = 8$), submitted to the amount of chemotherapy $v^*_{high} = 17.41$ and $v^*_{low} = 16.1$.

5.4. **Patient 2.** As far as the second virtual patient is concerned we set:

$k(\frac{u}{\gamma}, \mathsf{s}) = \kappa_0 + (1-\mathsf{s})\frac{u}{\gamma}$, $\beta(\frac{u}{\gamma}, \mathsf{s}) = 1 + 6(1-\mathsf{s})\frac{u}{\gamma}$, $F(\frac{u}{\gamma}, \mathsf{s}) = F_0 + 0.5(1-\mathsf{s})\frac{u}{\gamma}$,
$L(\frac{u}{\gamma}, \mathsf{s}) = L_0 + 8(1-\mathsf{s})\frac{u}{\gamma}$, $J = 0.007$, $F_0 = 0.3$, and $L_0 = 0.3$.

The tumor area is centered at $(0, 0)$ and is delimited by a circle of radius $r = 1.5$.

5.4.1. *Swanson's protocol.* In Figure 5, we take $v = 2$, $u_0(x, y) = 3\,.\,10^5$, $\varphi_0 = 1.82$, $\psi_0 = 2.29$ $(\varphi_0 + \psi_0 = 4.11)$ inside the tumor area and $u_0(x, y) = 0$, $\varphi_0 = 0.8$,

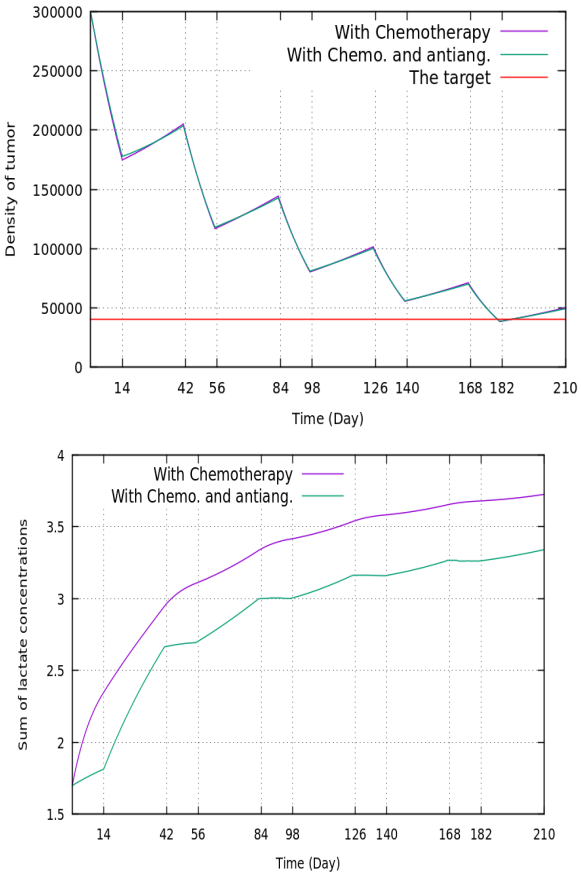

FIGURE 2. Patient 1, Evolution of the tumor and the lactates concentrations, with optimal chemotherapy ($v^* = 5.72$ if chemotherapy only and $v^* = 5.47$ if chemotherapy and antiangionenic/antiepileptic treatments)

$\psi_0 = 0.5$ ($\varphi_0 + \psi_0 = 1.3$) outside the tumor area. We compare the evolution of the tumor cell densities and of the sum of the lactate concentrations at the point $(0, 0)$ in four different cases: no treatment during the 30 weeks, only a chemotherapy treatment, only an antiangiogenic/antiepileptic treatment, and the combination of chemotherapy and antiangiogenic/antiepileptic treatments.

Now we take $u_0 = 6.10^5$, $\varphi_0 = 1.82$, $\psi_0 = 2.29$ ($\varphi_0 + \psi_0 = 4.11$) inside the tumor area and $u_0(x, y) = 0$, $\varphi_0 = 0.8$, $\psi_0 = 0.5$ ($\varphi_0 + \psi_0 = 1.3$) outside the tumor area. We search for the minimal amount of chemotherapy required for reducing the tumor cell density to $u_\Omega = u_Q = 10^5$. We get $v^* = 6.82$ when the chemotherapy is the only treatment ($\mathsf{s} = 0$), whereas the dose is smaller, $v^* = 6.57$, when the chemotherapy is combined with an antiangiogenic/antiepileptic treatment ($\mathsf{s} = 0.9$). Figure 6 displays the evolution of the tumor (above) and the lactate (below), submitted to the optimal quantities of chemotherapy in both therapeutic strategies. We see that the trajectories of the tumor cell densities coincide, whereas the trajectories of the lactate concentrations are lower when the treatment combines a chemotherapy and an antiangiogenic/antiepileptic drug.

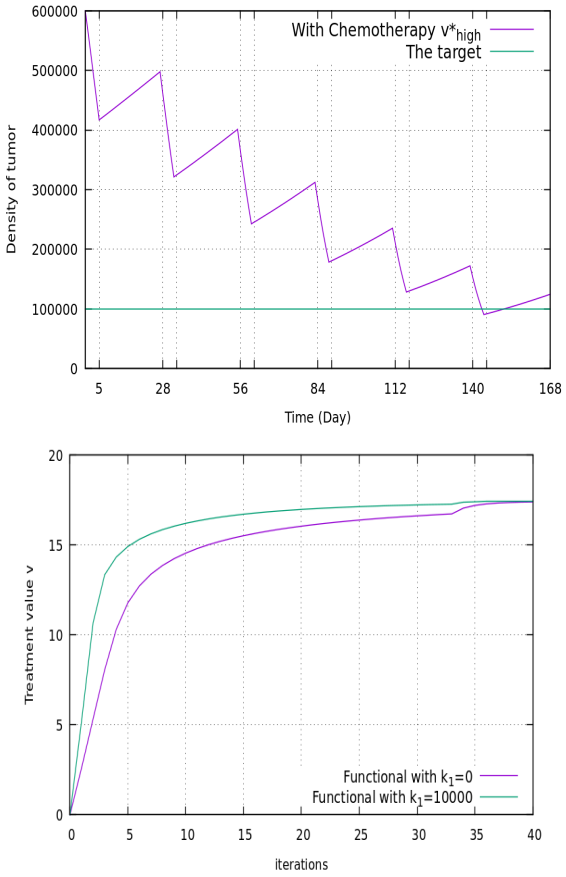

FIGURE 3. Patient 1, Evolution of the tumor concentration, with optimal chemotherapy ($v^* = 17.41$) (above); convergence of the algorithm to the optimal chemotherapy for two different choices of the functional $\mathcal{J}$ (below)

5.4.2. *Stupp's protocol.* The Figure 7 displays trajectories of the tumor cell densities and of lactate concentrations similar to those of Figure 6, the only difference being that this time the Stupp's protocol is used. We obtain $v^* = 15.19$ with the sole chemotherapy treatment, and $v^* = 14.9$ when the antiangiogenic/antiepileptic treatment supplements the chemotherapy. The Figure 8 displays the brain surrounding the tumor before the therapy (left) and at the end of the treatment, namely the Stupp's protocol with optimal chemotherapy and antiangiogenic/antiepileptic treatment (right).

Appendix. In this Appendix, for the reader's convenience, we report the computations leading to system (9) so that we can see, in particular, that (10) and (11) hold true. We preliminarily observe that, thanks to a generalization of Mean Value Theorem proved in [10, Appendix], being a and g are of class C^1, there exist measurable functions x^μ, y^μ, lying between $\varphi^\mu + \psi^\mu$ and $\varphi^* + \psi^*$, such that

$$g(\varphi^\mu + \psi^\mu) - g(\varphi^* + \psi^*) = g'(x^\mu)(\varphi^\mu + \psi^\mu - \varphi^* - \psi^*)$$

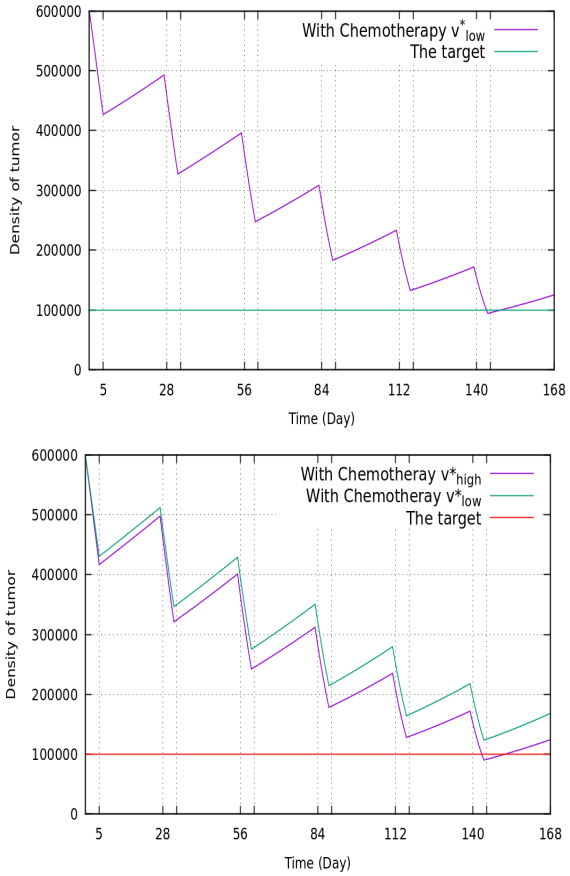

FIGURE 4. Patient 1 with low lactate level, evolution of the tumor with the optimal therapy $v_{low} = 16.1$ (above) ; Patient 1 with high lactate level, comparison of the trajectories of the tumor when the chemotherapy is dosed with v^*_{low} and v^*_{high} (below)

$$a(\varphi^\mu + \psi^\mu) - a(\varphi^* + \psi^*) = a'(y^\mu)(\varphi^\mu + \psi^\mu - \varphi^* - \psi^*).$$

In particular, x^μ, y^μ inherit the corresponding $L^\infty(\Omega_T)-$bounds from $\varphi^\mu + \psi^\mu$ and $\varphi^* + \psi^*$.

Analogously, there exist measurable functions η^μ, ω^μ, τ^μ, ζ^μ, ξ^μ, π^μ such that

$$\begin{aligned}
\mathrm{k}(\mathsf{s}^\mu) - \mathrm{k}(\mathsf{s}^*) &= \mathrm{k}'(\eta^\mu)(\mathsf{s}^\mu - \mathsf{s}^*) \\
p(\mathsf{s}^\mu) - p(\mathsf{s}^*) &= p'(\omega^\mu)(\mathsf{s}^\mu - \mathsf{s}^*) \\
\mathrm{F}(\mathsf{s}^\mu) - \mathrm{F}(\mathsf{s}^*) &= \mathrm{F}'(\tau^\mu)(\mathsf{s}^\mu - \mathsf{s}^*) \\
\mathrm{b}(\mathsf{s}^\mu) - \mathrm{b}(\mathsf{s}^*) &= \mathrm{b}'(\zeta^\mu)(\mathsf{s}^\mu - \mathsf{s}^*) \\
\kappa(u^\mu) - \kappa(u^*) &= \kappa'(\xi^\mu)(u^\mu - u^*) \\
L(u^\mu) - L(u^*) &= L'(\pi^\mu)(u^\mu - u^*).
\end{aligned}$$

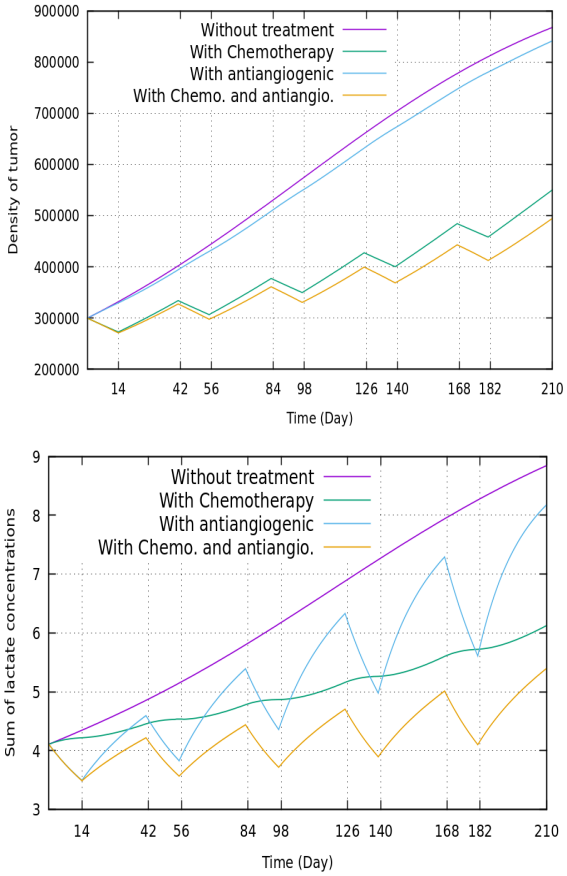

FIGURE 5. Patient 2, $v = 2$, Evolution of the tumor cell density (above) and the sum of lactate concentrations (below) with respect to time at the center of the tumor

Since the values of η^μ, ω^μ, τ^μ, ζ^μ are intermediate between those of s^* and s^μ, these functions are bounded in $L^\infty(\Omega_T)$. By the same argument, ξ^μ and π^μ lie between u^* and u^μ therefore they take values in $[0,1]$. Finally, there exist measurable functions λ^μ and ρ^μ such that

$$f_K(\varphi^\mu) - f_K(\varphi^*) = f'_K(\lambda^\mu)(\varphi^\mu - \varphi^*)$$
$$f_{K'}(\psi^\mu) - f_{K'}(\psi^*) = f'_{K'}(\rho^\mu)(\psi^\mu - \psi^*)$$

Again the values of λ^μ and ρ^μ lie between those of φ^* and φ^μ, while ρ^μ is intermediate between ψ^* and ψ^μ, yielding the corresponding $L^\infty(\Omega_T)-$bounds.

Taking advantage of the above formulae, we see that $Z^\mu = (Y^\mu, \Phi^\mu, \Psi^\mu)$ solves (9) that reads as

$$\begin{cases} \partial_t Y^\mu - \operatorname{div}[D\nabla Y^\mu] = A_1 Y^\mu + B_1 Y + A_2\Phi^\mu + B_2\Phi + A_3\Psi^\mu + B_3\Psi + C_0\mathsf{v} + C_1\mathsf{s} \\ \partial_t \Phi^\mu - \Delta\Phi^\mu = A_4 Y^\mu + B_4 Y + A_5\Phi^\mu + B_5\Phi + A_6\Psi^\mu + B_6\Psi \ + C_2\mathsf{s} \\ \partial_t \Psi^\mu - \Delta\Psi^\mu + F_0\Psi^\mu = A_7 Y^\mu + B_7 Y + A_8\Phi^\mu + B_8\Phi + A_9\Psi^\mu + B_9\Psi + C_3\mathsf{s}, \end{cases}$$

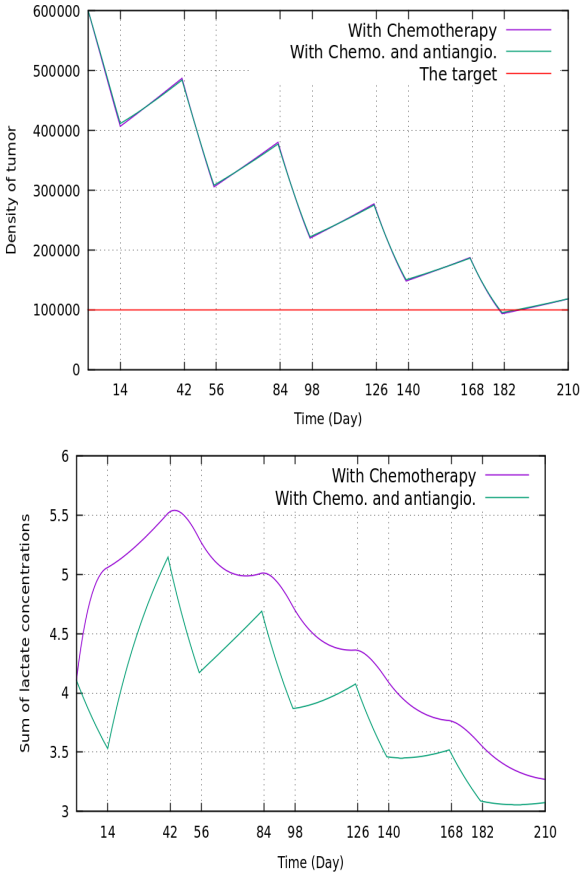

FIGURE 6. Patient 2, Evolution of the tumor and the lactates concentrations, with optimal chemotherapy ($v^* = 6.87$ if chemotherapy only and $v^* = 6.58$ if chemotherapy and antiangionenic/antiepileptic treatments)

where

$$C_0 = p(\mathsf{s}^*)[\kappa(u^\mu) - \kappa(u^*)]$$

$$C_1 = p'(\omega^\mu)\mathsf{v}^\mu\kappa(u^\mu) - p'(\mathsf{s}^*)\mathsf{v}^*\kappa(u^*)$$

$$C_2 = \mathrm{k}'(\eta^\mu)u^\mu[f_{K'}(\psi^\mu) - f_K(\varphi^\mu)] - \mathrm{k}'(\mathsf{s}^*)u^*[f_{K'}(\psi^*) - f_K(\varphi^*)] + J[\mathrm{b}'(\zeta^\mu)u^\mu - \mathrm{b}'(\mathsf{s}^*)u^*]$$

$$C_3 = \mathrm{F}'(\tau^\mu)u^\mu[L(u^\mu) - \psi^\mu] - \mathrm{F}'(\mathsf{s}^*)u^*[L(u^*) - \psi^*] + \mathrm{k}'(\eta^\mu)u^\mu[f_K(\varphi^\mu) - f_{K'}(\psi^\mu)] - \mathrm{k}'(\mathsf{s}^*)u^*[f_K(\varphi^*) - f_{K'}(\psi^*)].$$

The coefficients in the first equation above are

$$A_1 = [p(\mathsf{s}^*)\mathsf{v}^* - a^*]\kappa'(\xi^\mu) - g(\varphi^\mu + \psi^\mu)$$

$$B_1 = [p(\mathsf{s}^*)\mathsf{v}^* - a^*][\kappa'(\xi^\mu) - \kappa'(u^*)] - [g(\varphi^\mu + \psi^\mu) - g^*]$$

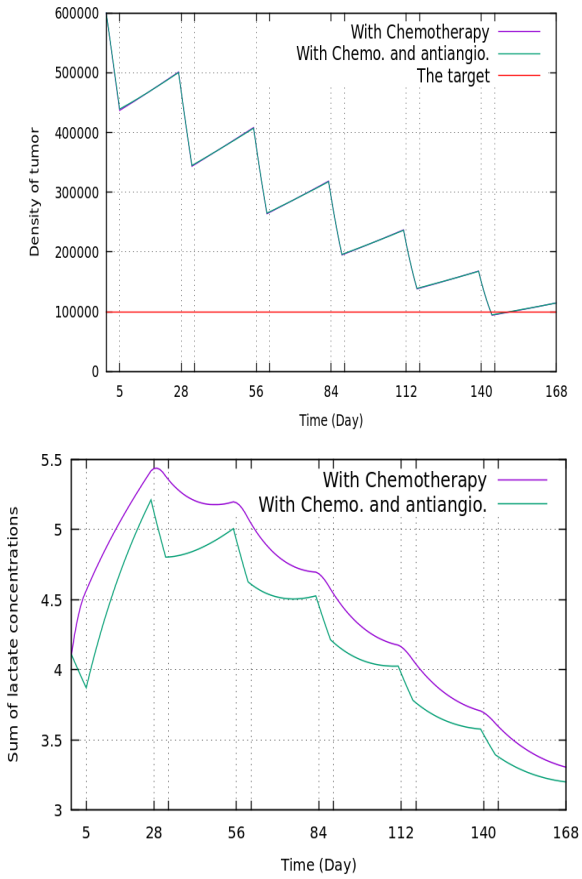

FIGURE 7. Patient 2, Evolution of the tumor and the lactates concentrations, with optimal chemotherapy ($v^* = 15.19$ if chemotherapy only and $v^* = 14.9$ if chemotherapy and antiangionenic/antiepileptic treatments)

$$A_2 = A_3 = -a'(y^\mu)\kappa(u^\mu) - u^* g'(x^\mu)$$
$$B_2 = B_3 = -[a'(y^\mu)\kappa(u^\mu) - a'^*\kappa(u^*)] - u^*[g'(x^\mu) - g'^*].$$

Here the superscript $*$ in a, g, a', g' means that the function is evaluated in $\varphi^* + \psi^*$. The coefficients in the second equation are

$$A_4 = -\mathrm{k}(\mathsf{s}^*)[f_K(\varphi^\mu) - f_{K'}(\psi^\mu)] + J\mathrm{b}(\mathsf{s}^*)$$
$$B_4 = \mathrm{k}(\mathsf{s}^*)[f_{K'}(\psi^\mu) - f_{K'}(\psi^*) - f_K(\varphi^\mu) + f_K(\varphi^*)]$$
$$A_5 = -k(\mathsf{s}^*, u^*) f'_K(\lambda^\mu)$$
$$B_5 = -k(\mathsf{s}^*, u^*)[f'_K(\lambda^\mu) - f'_K(\varphi^*)]$$
$$A_6 = k(\mathsf{s}^*, u^*) f'_{K'}(\rho^\mu)$$
$$B_6 = k(\mathsf{s}^*, u^*)[f'_{K'}(\rho^\mu) - f'_{K'}(\psi^*)].$$

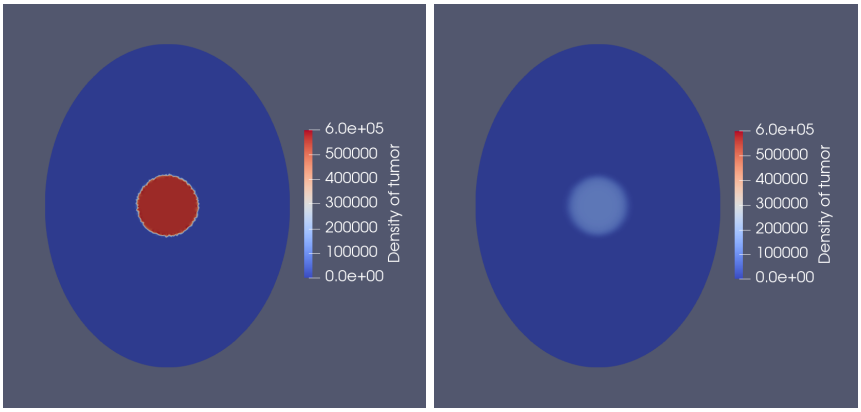

FIGURE 8. Patient 2, Brain surrounding the tumor before treatment (left) and at the end of treatment ($v^* = 14.9$, $\mathsf{s} = 0.9$)

Finally in the third equation we have

$$
\begin{aligned}
A_7 &= F_0 L'(\pi^\mu) + \mathrm{F}(\mathsf{s}^*)[L(u^\mu) + L'(\pi^\mu)u^* - \psi^\mu] + \mathrm{k}(\mathsf{s}^*)[f_K(\varphi^\mu) - f_{K'}(\psi^\mu)] \\
B_7 &= \mathrm{F}(\mathsf{s}^*)[L(u^\mu) - L(u^*) - \psi^\mu + \psi^*] + F(\mathsf{s}^*, u^*)[L'(\pi^\mu) - L'(u^*)] \\
&\quad + \mathrm{k}(\mathsf{s}^*)[f_K(\varphi^\mu) - f_K(\varphi^*) - f_{K'}(\psi^\mu) + f_{K'}(\psi^*)] \\
A_8 &= k(\mathsf{s}^*, u^*) f_K'(\lambda^\mu) \\
B_8 &= k(\mathsf{s}^*, u^*)[f_K'(\lambda^\mu) - f_K'(\varphi^*)] \\
A_9 &= -k(\mathsf{s}^*, u^*) f_{K'}'(\rho^\mu) - \mathrm{F}(\mathsf{s}^*)u^* \\
B_9 &= -k(\mathsf{s}^*, u^*)[f_{K'}'(\rho^\mu) - f_{K'}'(\psi^*)].
\end{aligned}
$$

Noticing that, due to (8),

$$
\begin{aligned}
&x^\mu, y^\mu \to \varphi^* + \psi^*,\ \lambda^\mu \to \varphi^*,\ \rho^\mu \to \psi^*,\ \pi^\mu, \xi^\mu \to u^*, \\
&\eta^\mu, \tau^\mu, \zeta^\mu, \omega^\mu \to \mathsf{s}^* \text{ in } C([0,T]; H),
\end{aligned}
\tag{19}
$$

then, being Lipschitz continuous all the involved nonlinearities by assumption, it is readily seen that

$\lim_{\mu \to 0^+} \|B_k\|_{L^2(0,T;H)} = 0$, for $k = 1, \dots, 9$, and $\lim_{\mu \to 0^+} \|C_j\|_{L^2(0,T;H)} = 0$, for $j = 0, \dots, 4$.

Besides, the $L^\infty(\Omega_T)$ bounds for the solutions together with the continuity of the nonlinearities yield $A_k, B_k \in L^\infty(\Omega_T)$ with

$$
\|A_k\|_{L^\infty(\Omega_T)} \le C_T, \quad k = 1, \dots, 9.
$$

Acknowledgments. Stefania Gatti was partially supported by the project NOBILI_PRIN2020 "Mathematics for industry 4.0 (Math4I4) 2020F3NCPX". Moreover, S. G. is member of G.N.A.M.P.A. of Istituto Nazionale di Alta Matematica I.N.d.A.M. Part of this work was done while S.G. was visiting the Laboratoire de Mathématiques et Applications at the Université de Poitiers, whose hospitality is gratefully acknowledged.

REFERENCES

[1] J. C. L. Alfonso, K. Talkenberger, M. Seifert, B. Klink, A. Hawkins-Daarud, K. R. Swanson, H. Hatzikirou and A. Deutsch, The biology and mathematical modelling of glioma invasion: A review, *J. R. Soc. Interface*, **14** (2017), 20170490.

[2] H. Alsayed, H. Fakih, A. Miranville and A. Wehbe, On an optimal control problem describing lactate production inhibition, *Applicable Analysis*, **102** (2023), 1711-1731.

[3] A. Aubert, R. Costalat, P. J. Magistretti and L. Pellerin, Brain lactate kinetics: Modeling evidence for neuronal lactate uptake upon activation, *Proceedings of the National Academy of Sciences of the United States of America*, **102** (2005), 16448-16453.

[4] M. U. Bogdańska, M. Bodnar, ...and V. M. Pérez-García, A mathematical model of low grade gliomas treated with temozolomide and its therapeutical implications, *Mathematical Biosciences*, **288** (2017), 1-13.

[5] J. F. Bonnans, J.-C. Gilbert, C. Lemaréchal and C. Sagastizábal, *Optimisation Numérique: Aspects Théoriques et Pratiques (Mathématiques et Applications)*, Springer, 1997.

[6] J. Chen, Y. Zhu, C. Wu and J. Shi, Engineering lactate-modulating nanomedicines for cancer therapy, *Chem. Soc. Rev.*, **52** (2023), 973-1000.

[7] L. Cherfils, S. Gatti, C. Guillevin, A. Miranville and R. Guillevin, On a tumor growth model with brain lactate kinetics, *Mathematical Medicine and Biology: A Journal of the IMA*, **39** (2022), 382-409.

[8] L. Cherfils, S. Gatti, A. Miranville and R. Guillevin, Analysis of a model for tumor growth and lactate exchanges in a glioma, *Discrete Cont. Dyn. Sys. S*, **14** (2021), 2729-2749.

[9] P. Colli, H. Gomez, G. Lorenzo, G. Marinoschi, A. Reali and E. Rocca, Mathematical analysis and simulation study of a phase-field model of prostate cancer growth with chemotherapy and antiangiogenic therapy effects, *Math. Models Methods Appl. Sci.,* **30** (2020), 1253-1295.

[10] P. Colli, H. Gomez, G. Lorenzo, G. Marinoschi, A. Reali and E. Rocca, Optimal control of cytotoxic and antiangiogenic therapies on prostate cancer growth, *Mathematical Models and Methods in Applied Sciences*, **31** (2021), 1419-1468.

[11] M. Conti, S. Gatti and A. Miranville, Mathematical analysis of a phase-field model of brain cancers with chemotherapy and antiangiogenic therapy effects, *AIMS Mathematics*, **7** (2022), 1536-1561.

[12] H. Garcke, K. F. Lam and E. Rocca, Optimal control of treatment time in a diffuse interface model of tumor growth, *Appl. Math. Optim.*, **78** (2018), 495-544.

[13] H. Gomez, Quantitative analysis of the proliferative-to-invasive transition of hypoxic glioma cells, *Integr. Biol.*, **9** (2017), 257-262.

[14] C. Guillevin, R. Guillevin, A. Miranville and A. Perillat-Mercerot, Analysis of a mathematical model for brain lactate kinetics, *Mathematical Biosciences and Engineering*, **15** (2018), 1225-1242.

[15] J. Guyon, I. Fernadez-Moncada, C. Larrieu, ... and T. Daubon, Lactate dehydrogenases promote glioblastoma growth and invasion via a metabolic symbiosis, *EMBO Molecular Medicine*, e15343, 2022.

[16] O. A. Ladyzenskaja, V. A. Solonnikov and N. N. Uralceva, *Linear and Quasi-linear Equations of Parabolic Type*, Vol. 23, Translations of Mathematical Monographs, American Mathematical Society, 1968.

[17] L. Li, A. Miranville and R. Guillevin, Cahn-Hilliard models for glial cells, *Appl. Math. Optim.*, **84** (2021), 1821-1842.

[18] J.-L. Lions, *Équations Différentielles Opérationnelles at Problémes aux Limites non Linéares*, Springer-Verlag, Berlin/Göttingen/Heidelberg, Germany, 1961.

[19] H. Raad, L. Cherfils, C. Allery and R. Guillevin, Optimal control of a model for brain lactate kinetics, *Asymptotic Analysis*, **133** (2023), 555-586.

[20] P. Sonveaux, F. Végran, ... and M. W. Dewhirst, Targeting lactate-fueled respiration selectively kills hypoxix tumor cells in mice, *J. Clin Invest.*, **118** (2008), 3930-3942.

[21] R. Stupp, W. P. Mason, et al., Radiotherapy plus concomitant and adjuvant temozolomide for glioblastoma, *The New England Journal of Medecine*, **352** (2005), 223-237.

[22] K. R. Swanson, E. C. Alvord and J. D. Murray, Quantifying efficacy of chemotherapy of brain tumors with homogeneous and heterogeneous drug delivery, *Acta Biotheor.*, **50** (2002), 223-237.

[23] K. R. Swanson, R. C. Rostornily and E. C. Alvord, A mathematical modelling tool for predicting survival of individual patients following resection of glioblastoma: a proof of principle, *Br. J. Cancer*, **98** (2008), 113-119.
[24] Y. Tang, C. Jia, Y. Wang, W. Wan, H. Li, G. Huang and X. Zhang, Lactate consumption via cascaded enzymes combined VEGF siRNA for synergistic anti-proliferation and anti-angiogenesis therapy of tumors, *Adv. Healthcare Mater.*, **10** (2021), 2100799.
[25] F. Troltzsch, *Optimal Control of Partial Differential Equations*, in Graduate Studies in Mathematics, 112. American Mathematical Society, Providence, RI, 2010.

Received for publication May 2023; early access March 2024.